

# Modification of Spacecraft Potentials by Plasma Emission

Richard Christopher Olsen\*

*The University of Alabama in Huntsville, Huntsville, Ala.*

The ion engine operations on Applied Technology Satellite 6 (ATS-6) altered the charge state of the spacecraft, changing the spacecraft surface potentials with respect to the distant plasmas. Plasma emission in quiet environments (plasma temperatures below 1 keV) caused the spacecraft potential to shift from a few volts positive to a few volts negative. A net ion current is emitted in such cases. The emission of a plasma or beam in energetic environments (plasma temperatures in the 5-10-keV range) in sunlight caused larger changes. Typical equilibrium potentials for ATS-6 in such environments were on the order of a hundred volts negative, with variations in potential across the spacecraft surface of comparable magnitude. Engine operations under such conditions raised the mainframe potential to near zero volts, and discharged the differential potentials on the dielectric surfaces. Plasma emission by the plasma bridge was an effective method of discharging kilovolt potentials in eclipse.

## Introduction

**A**PLIED Technology Satellite 6 (ATS-6) carried twin cesium thrusters designed to test ion engine technology and to test their usefulness for stationkeeping on the three-axis-stabilized satellite. They performed successfully, demonstrating thrust, an absence of interference with spacecraft systems, and beneficial effects on spacecraft potentials. In addition, the plasma bridge neutralizers were successfully operated in special operations in 1976 and 1977 to observe the changes in spacecraft potentials caused by plasma emission.

The operations of the ion engine have been studied with an emphasis on the effects of plasma emission on the spacecraft mainframe potential and surface potentials. This analysis was motivated by a desire to determine the usefulness of plasma emission as a means of controlling spacecraft charging. ATS-6 provided a large data set on spacecraft charging in sunlight and eclipse, and these experiments in potential modification rest on a large background of charging studies.

The main motivation for this study is a desire to understand the effect of beam and plasma emission on the electrostatic configuration of the spacecraft. This is important not only for thruster design, but also for controlling spacecraft charging at geosynchronous altitude.

Nonzero spacecraft potentials have been noted since the beginning of satellite flights. Large negative potentials (hundreds to thousands of volts) were first observed on ATS-5 in eclipse.<sup>1</sup> These were explained as the natural result of a balance of the ambient electron and ion currents with associated secondary electron currents. In sunlight, photoemission normally provides a large enough current to preclude negative spacecraft potentials. It was therefore difficult to explain the negative potentials found in sunlight, first on ATS-5, and then on ATS-6.<sup>2,3</sup> This problem gained importance when it became clear that there was an association between spacecraft charging and anomalies in spacecraft behavior.<sup>4</sup> Further study of the daylight charging phenomena on ATS-6 showed the existence of an electrostatic barrier around the science package, and it was postulated that differential charging of insulators might be the cause.<sup>5</sup> It was eventually shown that the large dish antenna, Fig. 1, was responsible for the barrier around the instrument package.<sup>6</sup> The charging process has been modeled by a three-dimensional computer code capable of calculating the electric field distribution around an object and the resulting currents

to that object. This code was applied to a Teflon sphere model in a magnetospheric environment and it was found that as the shadowed surfaces charged negatively, the resulting field distribution was such as to limit photoemission from the illuminated side. Once an electrostatic barrier was established, the object as a whole charged negatively, maintaining the differential potential.<sup>7</sup>

Relatively few reports on plasma emission in space have been published. The Space Electric Rocket Test 2 (SERT-2) flight at 1000 km showed the ion beam was effectively charge and current neutralized by the plasma bridge neutralizers, but the data taken there are not directly applicable to the problem of charging at higher altitudes. The results of the early ATS-6 engine operations have been published, along with a preliminary look at the effects of particle emission on the spacecraft potentials.<sup>9,10</sup> It was found that plasma emission could control the negative potentials ordinarily found in sunlight, though the physics of the charging process on the satellite was still not understood well enough to permit an explanation of the emission effects.

In the sections which follow, the ion engine and particle detectors are described, then the results of engine operations in quiet and energetic environments. The first examples are for operations in sunlight, with a concluding example of the effect of plasma emission on a negatively charged satellite in eclipse.

## Spacecraft Description

ATS-6 was launched on May 30, 1974 into geosynchronous orbit with a full payload of scientific and engineering experiments, particularly communications experiments. The

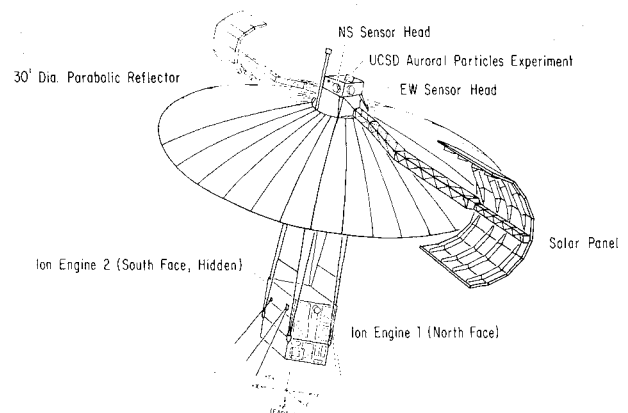


Fig. 1 ATS-6 spacecraft, ion engines and detectors.

Received Nov. 11, 1980; revision received April 27, 1981. Copyright © American Institute of Aeronautics and Astronautics, Inc., 1981. All rights reserved.

\*Research Associate, Department of Physics. Member AIAA.

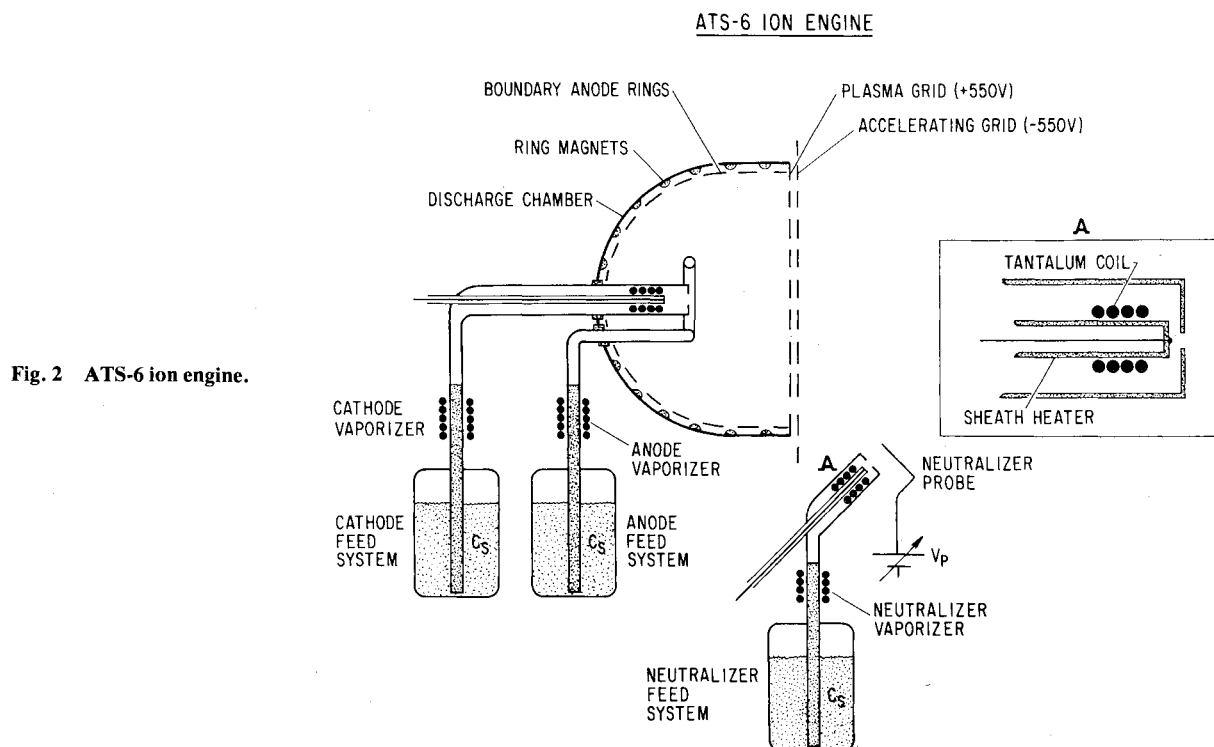


Fig. 2 ATS-6 ion engine.

spacecraft is illustrated in Fig. 1, with the Environmental Measurements Experiment (EME) package shown at the top, the large dish antenna and solar arrays extending outward, and the Earth Viewing Module (EVM) at the focus of the antenna. The ion engine experiment was located on the EVM, with complete assemblies on the north and south faces of the EVM. The plasma detector was located on an outer corner of the EME package, and thus physically separated from the ion engine by 10 m and by the dish antenna. The mesh antenna is transparent to charged particles, however, and is a barrier to ion motion only when positively charged. It is constructed from a Dacron mesh which was copper flashed, and then coated with a silicon lubricant to aid in thermal control and deployment. It is therefore an insulator and capable of charging with respect to the mainframe.

#### Ion Engine Description

The thruster design is illustrated in Fig. 2. The discharge chamber utilized the magnetoelectrostatic (MES) concept, in which the magnetic and electric fields in the chamber constrain the plasma. Two parallel grids are used to extract the plasma, with the outer accelerator grid at  $-550$  V and the inner screen grid at  $+550$  V. The 8-cm-diam thruster produced 4.5 mN thrust, with 0.1 A of cesium ions at a final kinetic energy of 550 eV.<sup>9</sup>

The plasma bridge neutralizer is necessary to provide charge and current balance for the main beam and is an excellent plasma source by itself. The neutralizer emission modes have a large effect on the spacecraft potentials. The cathode is located 5.0 cm downstream from the accelerator electrode, and points 60 deg downstream. The hollow cathode is provided with an auxiliary electrode, or probe, slightly above the cathode. In operation, cesium is fed through the cathode, and an arc is struck between the probe and cathode. The probe is initially held at  $+150$  V with respect to the neutralizer, then drops in potential as current begins to flow.

The emission characteristics of the neutralizer vary with cathode temperature and cesium flow rate. At low cathode temperatures (typically in startup), operation is in a low emission current, high extraction voltage mode named plume mode, for the appearance of the discharge. Once the cathode heats up, the cesium flow rate increases and the plasma bridge

enters spot mode. Spot mode is characterized by high emission currents at low extraction voltages. The neutralizer can provide substantial electron current in either mode, but does not become an efficient ion source until spot mode.

We will see that the equilibrium condition when the ion engine is operating is to have a negative spacecraft potential of a few volts. The coupling between the neutralizer and the beam gives a potential difference between the beam and the spacecraft between 4 and 7 V, which implies the beam potential is near zero volts with respect to the ambient plasma.

#### Detector Description

The plasma detector was designed to measure the ambient particle population from 1 eV to 80 keV in energy, as a function of energy, time, and angle. Two detector heads rotated in orthogonal planes, and each head contained paired ion and electron detectors. An additional ion detector was fixed to the EVM/EME frame. One scan in energy requires 16 s, one rotational sweep requires 2½ min. Detector angles are defined such that 90 deg corresponds to looking radially away from the spacecraft, or straight "up."<sup>11</sup>

#### Ion Engine 2, Thruster Operation

The first ion engine operation was on July 18, 1974. This data set shows the effects of plasma emission on a spacecraft that is initially positively charged. The data taken on this day are unique for a number of reasons besides the ion engine operation. The satellite is in the Earth's midnight region, normally an environment of hot (keV) plasmas. The environment was unusually quiet on this day, with the magnetic activity index,  $\Sigma K_p = 12+$ , and no injections of hot plasmas (i.e., substorms) during the day. The previous day was also quiet, with  $\Sigma K_p = 16+$ , and the 3-h  $K_p$  at the time of operation was 2. Because the magnetosphere was quiet for an extended time period, the environment was an unusually cool, dense plasma. The detectors were in a good mode for this study, with excellent low-energy coverage.

Six hours of data are shown from the north-south detector in Fig. 3. The spectrogram format used here is a gray scale presentation of the particle fluxes observed as a function of time. The intensity plotted is proportional to the flux, with higher fluxes plotted as lighter grays. The horizontal axis is

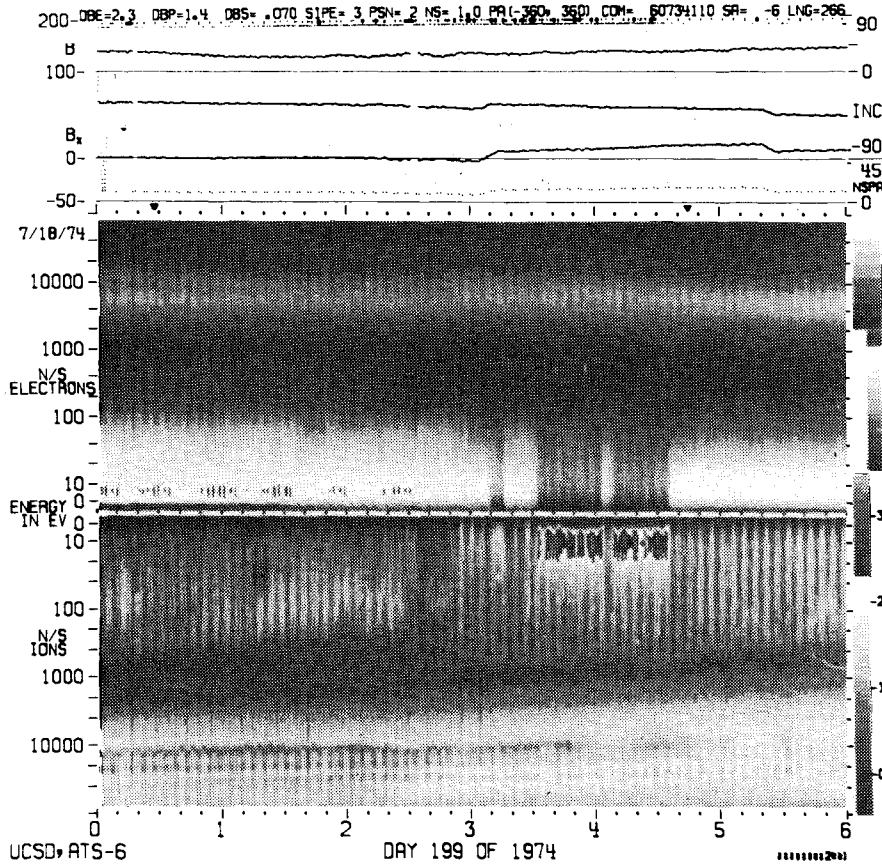


Fig. 3 Spectrogram, July 18, 1974.

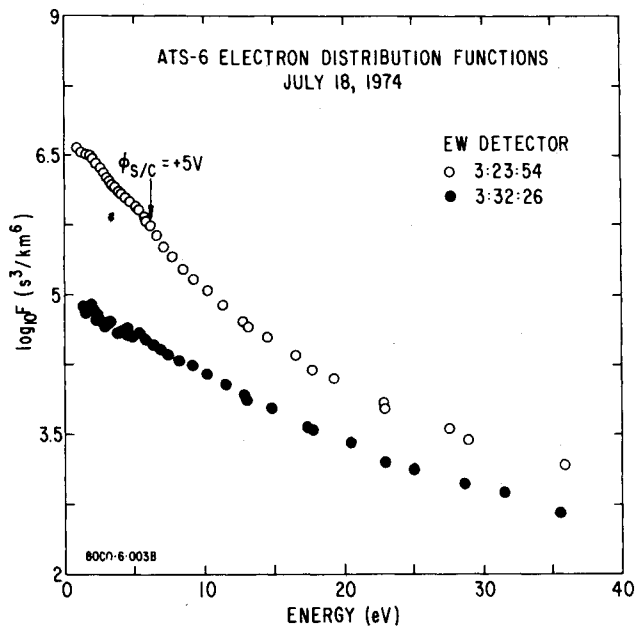


Fig. 4 Electron distribution functions, July 18, 1974.

universal time in hours and minutes; the vertical axes are the particle energies (per unit charge). Both energy scales have their zeros in the middle of the plot. A strong pitch angle dependence in the ion population is found in the north-south detector data before the operation begins. Data from the east-west head show a thermal ion population perpendicular to the magnetic field which becomes more apparent when the engine is operated. During the operations, the bright band of low-energy electrons (0-40 eV) darkens considerably signaling a shift in the spacecraft potential. This can be seen during the neutralizer operation from 03:10 to 03:15, and during the main thruster operations from 03:32 to 04:03 and 04:08 to

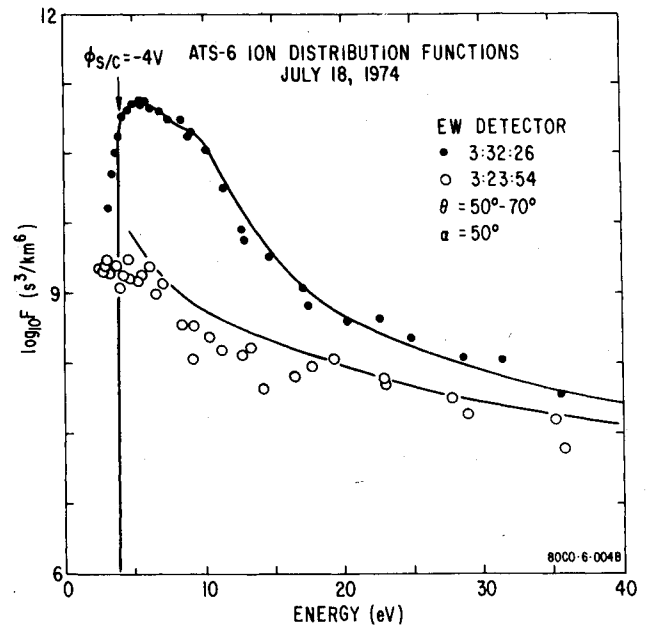


Fig. 5 Ion distribution functions, July 18, 1974.

04:35. The intensification of ion fluxes at these times is also due to the potential shift.

The distribution functions from before and during the operation provide some details of the ion engine effects. Figures 4 and 5 show the electron and ion distribution functions for 03:24 (engine off) and 03:32 (engine on) from the east-west detector. The electron data at 03:24 show a break at 5 eV, suggesting a boundary between spacecraft-generated electrons (photoelectrons) and the ambient population, and thus a +5 V potential. The electrons below the break are characterized by a temperature of 2.45 eV and a density of  $27.8 \text{ cm}^{-3}$ , as determined by a least-squares fit of the 2.0-5.0-

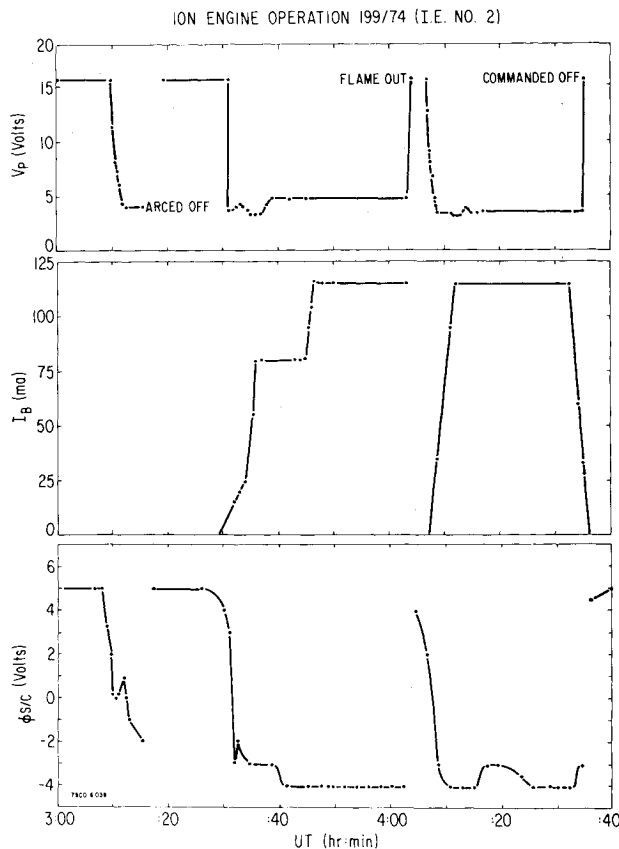


Fig. 6 Ion engine operation, July 18, 1974.

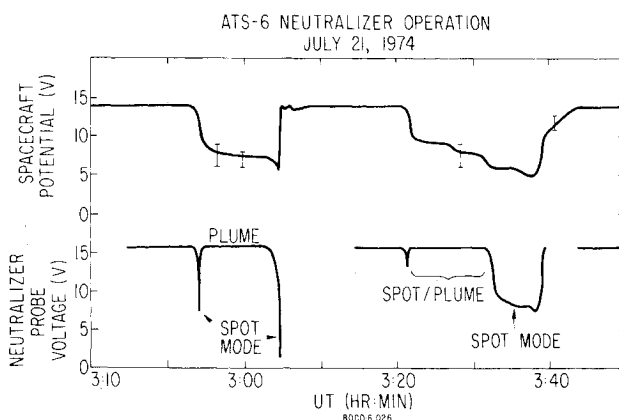


Fig. 7 Plasma bridge operation, July 21, 1974.

eV data. The ambient population has a temperature of 5 eV at low energies, and a density of 2 to 3  $\text{cm}^{-3}$ , depending on the spacecraft potential assumed in the calculation.

The 03:32 ion data show a sharp drop at 4 eV, giving a -4-V potential when the engine is on. A shift of 8 or 9 eV in the particle spectra in the appropriate directions bring them into agreement, showing that there has been an 8- or 9-V shift in the spacecraft potential. The absolute measurements and shift measurement give a comforting agreement.

The data were examined in this fashion throughout the operation period, and the resulting potentials are shown in Fig. 6. The neutralizer probe voltage is at the top of the plot. This measurement gives the status of the small plasma bridge, particularly denoting the beginning of spot mode operation. The beam current gives the status of the main thruster. The potential measurements at the bottom are subject to  $\pm 1$ -V uncertainties, with error bars left off to avoid clutter. Small fluctuations in potential are probably real.

The neutralizer operation resulted in a -1-V potential, while the full beam set the spacecraft to -4 V. The shift to

negative potentials implies a distinct change in the spacecraft current balance. More photoelectrons and secondary electrons will now escape, increasing the (inward) positive current to the spacecraft. The change in potential reduces the ambient electron flux and increases the ambient ion flux, again increasing the positive current to the spacecraft. These changes are balanced by a net ion current leaving the spacecraft through the beam. The small change in potential will primarily affect the thermal fluxes. The thermal electron flux has a 5-eV temperature and a density of 2  $\text{cm}^{-3}$ , while the ion population is mostly a 1-eV 2- $\text{cm}^{-3}$  hydrogen plasma. The secondary electron fluxes in this environment are a small percentage of the current balance. The photoelectron flux has a maximum value of  $1 \times 10^{10}/\text{cm}^2\text{-s}$ . This is reduced by a factor of 100 by the +5-V potential when the neutralizer is off.<sup>12</sup> The thermal fluxes for zero potential are about  $1 \times 10^8$  for the electrons and  $8 \times 10^5$  for the ions. The balance of currents gives a net ion flux from the neutralizer that basically equals the integrated photoelectron flux, about 1.6 mA assuming a 100- $\text{m}^2$  surface area (an extreme upper bound). The ion engine telemetry gives an upper bound of 3-5 mA on the net current emitted.

No signs of cesium ions being returned to the spacecraft were found.

### Ion Engine 2, Neutralizer Operations

The ion engines flooded at the ends of their initial tests, causing them to fail. The failure mode of the ion thrusters was not understood until long after the July operation of engine 2. Because of this, the restart attempts of the engine, with and without the neutralizer, continued until the power supply was so badly shorted out that it could not supply the necessary heater current to send the plasma bridge into spot mode. During the latter stages of the restart attempts, the transitions to spot mode came slowly, providing opportunities to study the time dependence of these transitions.

#### July 21, 1974

Operations on July 21 were again in a "quiet" environment, and the neutralizer did not cause major changes in the spacecraft potential. The spacecraft was positively charged when the neutralizer was off and was consistently pushed toward zero by the neutralizer.

This data set provides the best look at the relationship between spacecraft potential and the neutralizer status. The spacecraft potential must be inferred entirely from the electron data at this time because of the relatively large positive potential and an absence of visible ions. Breaks in the distribution functions imply the equilibrium spacecraft potential is +14 V when the neutralizer is off and +8 V in spot mode. (Note that the neutralizer does not fully reach spot mode, compare July 11.) Using the break in distribution functions and their shifts relative to each other, the potential was obtained as a function of time. Plotted in Fig. 7 along with the probe voltage, the strong dependence of the spacecraft potential on the neutralizer mode is apparent.

The spacecraft is driven toward zero by the neutralizer at 03:00 and 03:30 by the two operations. Although the probe voltage telemetry does not come on scale for much of this period, it appears that the neutralizer was on the edge of spot mode during the periods the spacecraft is partially discharged. This is the case from 02:55 to 03:05 and from 03:22 to 03:32. When the probe voltage drops to 5 or 10 V, and the neutralizer ion current increases, a further drop in the spacecraft potential occurs, as seen at 03:30. The neutralizer mode affects its ability to produce ions, and the ion current produced by the neutralizer determines the spacecraft potential.

### Ion Engine 1, Thruster Operation

#### October 19, 1974, Neutralizer and Thruster Ignition

The second successful ion engine operation began on October 19, 1974, and ran for 92 h. The environmental conditions at this time were considerably different from those

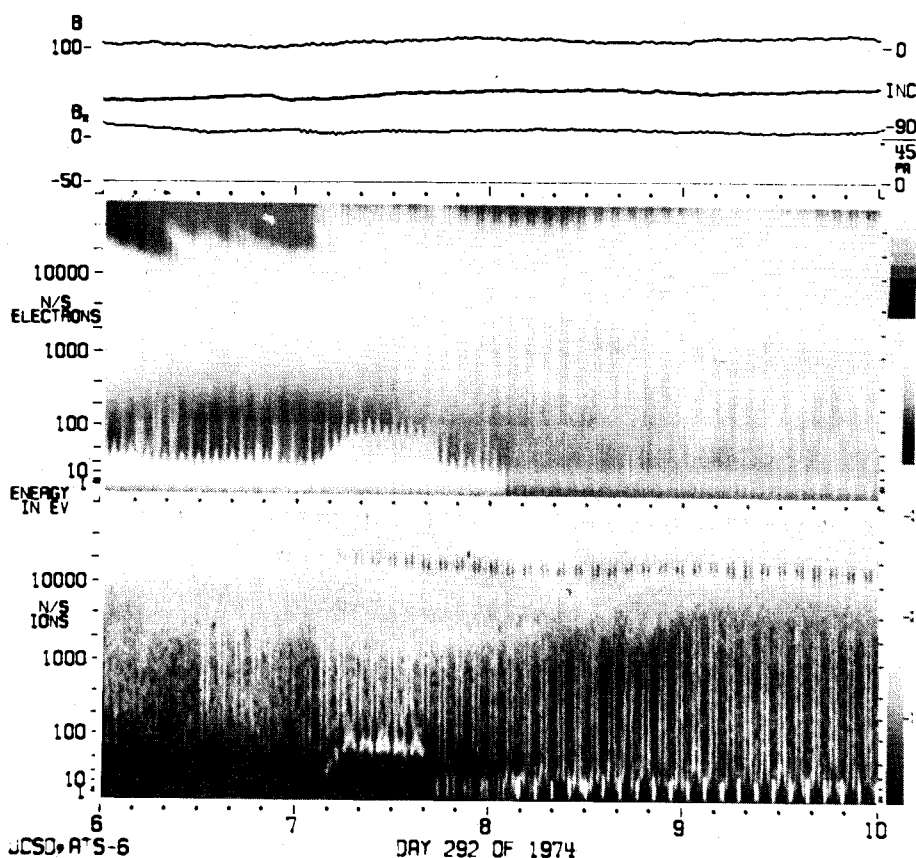


Fig. 8 Spectrogram, October 19, 1974.

found in the first test. The operation began in the midst of a substorm, 2 h after local midnight. This is a disturbed environment with negative spacecraft potentials and differential charging effects visible before the operation begins. Data are only available from the north-south detector head.

Four hours of data from the engine ignition period are shown in Fig. 8. Both energy scales increase upward on this spectrogram. The periodic structure in the particle data reflects the rotation of the detector head, the angular dependence of local charging effects, and the pitch angle variations in the ambient population. An injection event at 07:05 caused the spacecraft to charge to between  $-40$  and  $-50$  V and caused an increase in the height of the differential charging barrier to about 100 V by 07:15. The potential can be seen to rise to near zero at 07:40:43, when a series of short vertical lines appear in the low-energy (0-20 eV) ion data. At this time also, the differential charging barrier height drops, disappearing completely at 08:05.

The spacecraft potential and differential charging barrier height are given in Figs. 9 and 10. The spacecraft potential was measured by finding the lowest-energy ion channel with measurable counts and taking that as the spacecraft potential. This can lead to potential measurements which are too negative if there are too few ambient low-energy ions to measure. Data points were taken with the detector at 90 deg (straight up, away from the spacecraft) to minimize the effects of local fields. The measurement assumes that the observed ions are not generated on the spacecraft, which proved to be a good assumption at this angle. The barrier height was measured by examining the electron distribution function, and finding the break, or drop, where the transition from spacecraft-generated particles to ambient particles occurs. These measurements were also made at 90 deg. Both measurements are subject to about 10% error due to the width of the energy channels.

The plasma bridge enters spot mode at 07:41 and the spacecraft potential rises to about  $-3$  V. (The detector was at 170 deg at this time, so two data points at that position are

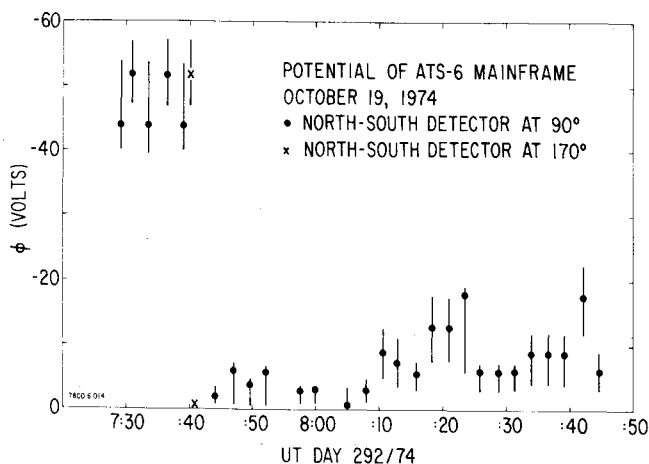


Fig. 9 Mainframe potential, October 19, 1974.

included in the plot.) The differential charging barrier falls to about 20 V from 100 V about 2 min later. The engine ignition at 08:00 causes a slight drop in potential, and then the disappearance of the differential charging barrier. The time dependence of the observed effects helps explain the physical phenomena that are occurring.

The other major piece of information in the particle data is the direction of the thermal ion fluxes. There is a peculiar effect to be noted in the angular distribution of the intense fluxes of low-energy (0-20 eV) ions seen after the neutralizer ignites.

These ions are neither isotropic nor field aligned, the usual angular distributions seen in this energy range at local midnight.<sup>13</sup> Close examination of the data at 08:26 and 08:28 on the spectrogram reveals field-aligned ions down to a few electron volts. These are not nearly as intense as the fluxes at other angles. Furthermore, the incidence angle of the intense fluxes changes with time, while the environment is almost

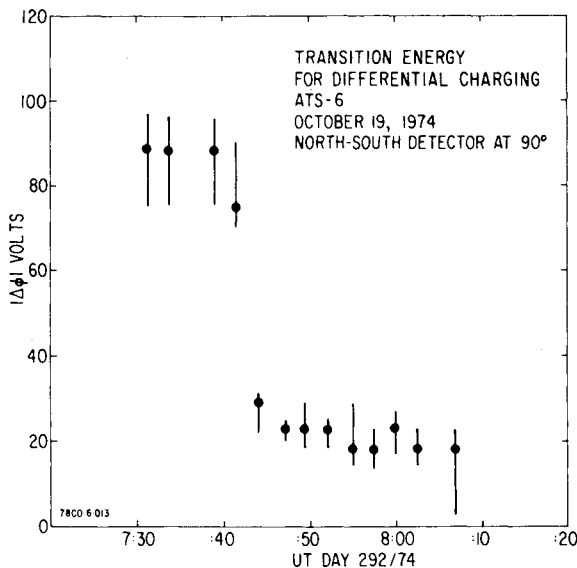


Fig. 10 Barrier height, October 19, 1974.

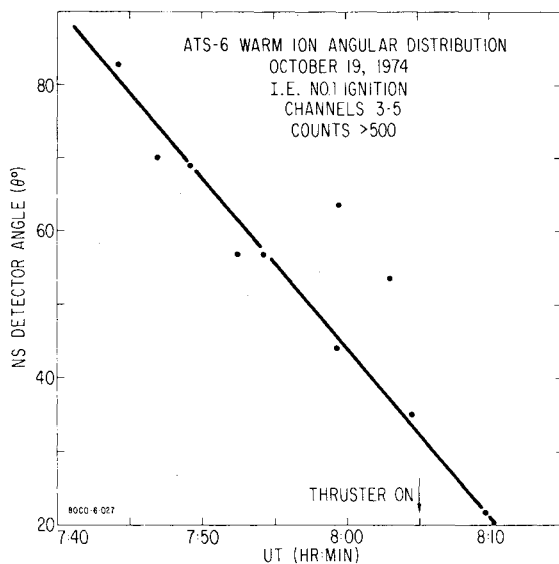


Fig. 11 Ion angular distribution, October 19, 1974.

constant. Figure 11 gives the incidence angle of the intense fluxes as a function of time. The intense fluxes initially appear at 83 deg spacecraft angle at 07:44, several minutes after the neutralizer enters spot mode. The incidence angle drops steadily until 08:10, when the thruster ignites, and stabilizes near 0 deg spacecraft angle thereafter. These fluxes must be cesium from the engine.

The change in the incidence angle of the intense fluxes reflects the changes in the local electric fields as the ion fluxes from the engine discharge the negative dielectrics on the top of the EVM, the antenna, and the solar arrays. In equilibrium, the incidence direction stabilizes at one end of the detector rotational pattern, with particles entering tangentially along the antenna and solar array strut.

The variations in spacecraft potential with time and the identification of low-energy ion fluxes from the engine provide the information necessary to describe the sequence of changes in the electrostatic configuration of the spacecraft. Initially, the sunlit spacecraft has a number of dielectric surfaces around the conducting spacecraft components which are negatively charged with respect to the spacecraft. This condition has been shown to be the normal response of the spacecraft to an energetic particle environment. The large dish antenna has been shown to be largely responsible for the barrier around the EME module.<sup>6</sup>

The insulators on the EVM (primarily the Kapton surface of the thermal blanket) serve a similar purpose there. These barriers are essential for the development of negative potentials in this environment. Emission of electrons only (at energies below the barrier height) will not discharge the satellite. For the spacecraft to be discharged, the differentially charged insulators must be brought closer to the mainframe potential. Once the barrier has been removed, an electron current from the neutralizer can escape and discharge the mainframe. Laboratory tests on hollow cathode devices show that the ion current extracted from a cathode depends on the extraction voltage and suggest that for potentials of tens of volts over 10-20 cm., currents of tens of microamps can be extracted.<sup>14</sup>

The likely sequence of events is as follows:

- 1) Negatively charged spacecraft has insulating surfaces which are negatively charged with respect to the main frame.
- 2) The neutralizer ignition into plume mode has no measurable effect on the spacecraft because the thermal electrons cannot push through the barrier around the EVM.
- 3) Spot mode operation of the neutralizer provides an ion source capable of discharging the EVM insulating surfaces which were limiting the emission of photoelectrons and secondary electrons from the conducting surfaces of the EVM. This alone probably would be sufficient to discharge the satellite.
- 4) The neutralizer provides an electron current as necessary to raise the spacecraft potential to  $-1$  to  $-3$  V.
- 5) Ion fluxes from the neutralizer partially discharge the antenna, but do not complete the process. The extraction field is apparently not high enough to draw sufficient current.
- 6) The engine ignites, causing a shift in the operating mode of the neutralizer and providing a large flux of charge exchange ions. These ions complete the discharge of the dielectrics, leaving only sufficient potentials to maintain the ion flux to the dielectric surfaces.

#### October 19-23, 1974—Engine Steady State

The engine ignition process discussed in the previous section was followed by 92 h of uneventful (from an engineering viewpoint) operation. After examination of the ignition sequence, this long operation provides a different sort of information, namely, the equilibrium behavior of this charging system.

The rotating detector head stuck early in the operation, and was pointed in the direction of the large ion flux. This did not hinder the measurements, however, and the data taken during this time show several interesting effects. Figure 12 is a 4.5-day spectrogram covering this time period. The bright band of ions can be seen to extend across most of the spectrogram. Indentations in the middle of the spectrogram at 18:00 of each day are an instrumental effect and reflect an absence of low-energy particle information at these times. The transition of the white band of ions to black seen at 0 to 4 UT on day 293 and 294 is an example of the cycling of the gray scale. The spacecraft was held at about  $-4$  V throughout this time period in spite of the great variety of environments the spacecraft passes through, including four large substorms. Remarkably, the night-side data are free of differential charging throughout this time period. Close study shows that differential charging effects generated no barrier above the 1-V level. This implies that fluxes of thermal ions were moving from the ion engine to the shadowed insulating surfaces which ordinarily charge negatively and cause a barrier to electrons. The operation of the thruster maintained the spacecraft near zero volts potential, eliminated the problem of differential charging, and as a result greatly improved the particle data.

#### Neutralizer Operations in Eclipse

As part of the program to study the effects of the ion engine on spacecraft potentials and to study means of modifying potentials, the ion engine neutralizers were operated during

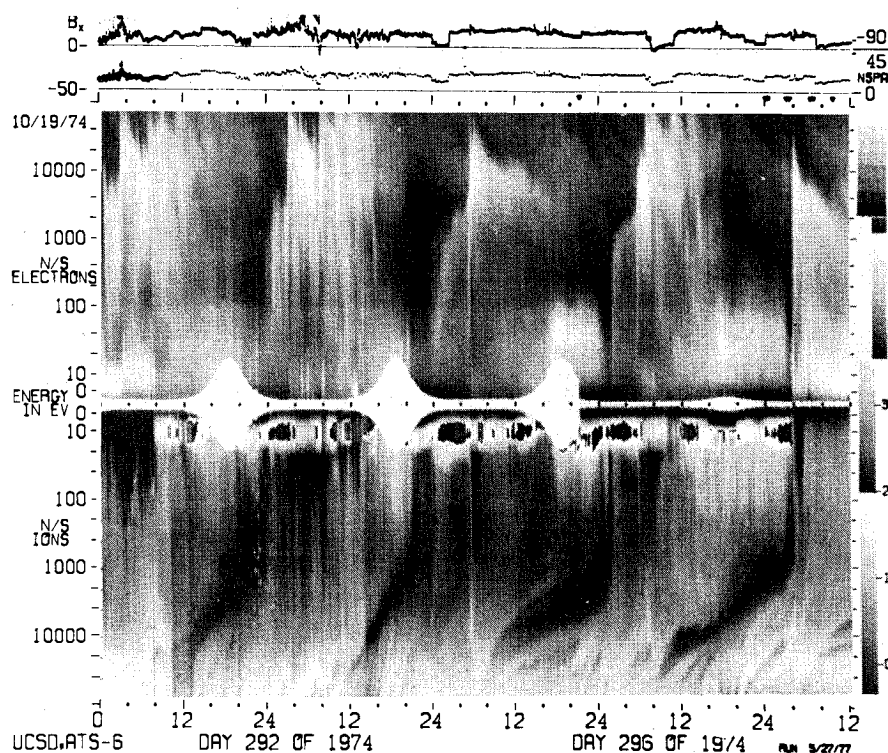


Fig. 12 Spectrogram, October 19-23, 1974.

periods of spacecraft eclipses. ATS-6 was normally at a positive potential in sunlight in quiet environments. If the positive spacecraft then entered eclipse, the particle data usually showed a small shift in the negative direction as the photoelectric current was cut off. The equilibrium potential in such eclipses was generally between +1 and -3 V. In energetic environments, the sunlit satellite was generally tens of volts negative to as much as 1 kV negative. Under such conditions, an eclipsed satellite normally charged to several kilovolts negative.

Analysis of the neutralizer operations associated with the full thruster tests suggest that the neutralizer should do as thorough a job of controlling the spacecraft potential in eclipse as it did in sunlight.

When operated at quiet times in eclipse (no large negative potentials) a small ion current from the neutralizer caused a shift of a few volts in the negative direction. In more active environments, larger charges were seen.

#### April 7, 1977

Two operations in April 1977 showed that if the spacecraft was charged several kilovolts negative, the neutralizer would discharge the satellite. Figure 13 shows the results from April 7, 1977. The solar array current reflects the illumination of the spacecraft, the neutralizer probe voltage shows its status, and the potential at the bottom comes from ion data. The spacecraft charges to -3 kV in eclipse from 09:05 to 09:15, and the potential rises to near zero at 09:15 when the neutralizer ignites. The neutralizer is an excellent electron source even in plume mode, and the absence of differential charging in this case means that ions are not needed in such abundance. The spacecraft remains near zero potential until the neutralizer is switched off at 09:33. At this time, the spacecraft potential falls to -1.5 kV for the few minutes remaining in eclipse. Neutralizer operation has provided the necessary electron current to discharge the satellite and maintain it at low potentials. This is in contrast to the observed results of filament emission of electrons on ATS-5. Experiments on ATS-5 showed that the ability of the filament emitter to discharge the satellite was extremely limited and that it could not hold the spacecraft at low potentials. Analysis showed this was due to differential charging of the spacecraft insulators and a barrier to electron emission. The

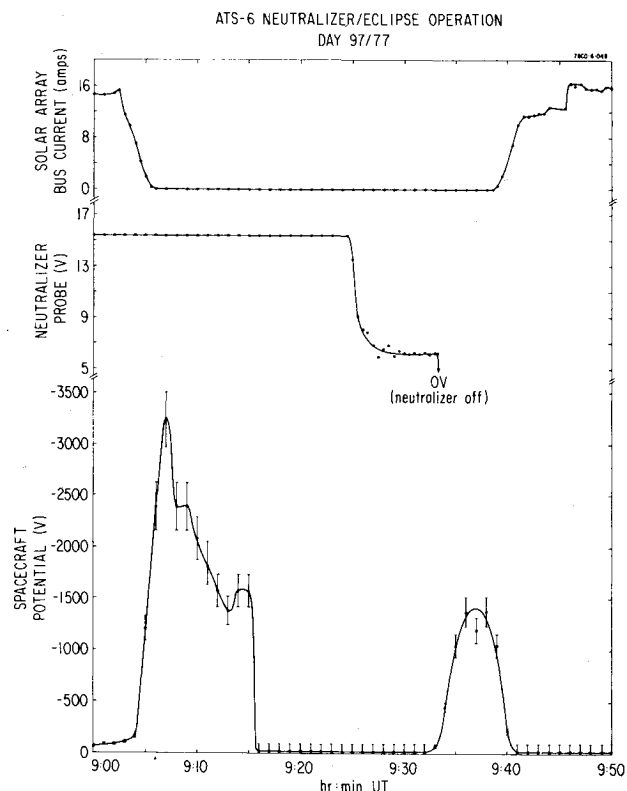


Fig. 13 Plasma bridge operation, April 7, 1977.

difference is the presence of ions in the plasma which can discharge the dielectrics and hold them near the mainframe potential.<sup>10,15</sup>

#### Summary

Operation of the ion engines and plasma bridge neutralizers had major effects on the spacecraft potential with respect to the ambient plasma and on the differential potentials on the spacecraft surfaces. The neutralizer or the engine could discharge large negative potentials at all times. Differential charging was reduced by the neutralizer when operated in spot



mode, i.e., as an ion source, and eliminated by operation of the ion engine.

The operation of the neutralizer or the main thruster in a quiet environment resulted in the production of a net ion current by the engine, sufficient to drive the spacecraft slightly negative. Moving into eclipse changed the amount of ion current being supplied by the neutralizer.

When the neutralizer was used in daylight cases of negative charging, i.e., in active environments, the neutralizer caused the spacecraft to rise to a few volts negative potential and the reduction of differential charging on the insulating surfaces of the spacecraft. Operation of the thruster in active environments held the spacecraft at  $-4$  to  $-5$  V potential and eliminated the problem of differential charging. Fluxes of ions were seen from the engine and neutralizer when the spacecraft was in active environments.

The ion engine operations analyzed here show that plasma emission can be used to control spacecraft charging and does not generate differential potentials as electron emission does. A plasma source designed to control charging on a geosynchronous satellite needs to provide a sufficient current of thermal ions to hold shadowed dielectrics near the mainframe potential and a sufficient current of electrons to hold the mainframe near zero volts in eclipse. Plasma bridge design has not generally concentrated on optimization as an ion source, but it appears that even the standard design used for ATS-6 or SERT 2 is adequate.<sup>14,16,17</sup> In the ATS-6 data set, it appears that 1 mA is adequate to control the spacecraft potential. The bias of the plasma source will determine the potential of the spacecraft within certain limits. If the source is driven negative with respect to the spacecraft, in an attempt to drive the spacecraft positive, the electron current drawn from the source to the spacecraft grows excessive. Biasing the source a few volts positive with respect to the spacecraft, as in the case of ATS-6, seems to be optimum for maintaining an ion current out toward the dielectric surfaces. Development of plasma sources for potential control needs to be concentrated in the area of optimizing the plasma bridge, or a similar device, as an ion source with constraints of fuel and power usage. This work indicates a relatively small ion contamination flux arriving on the spacecraft, but worries about contamination are probably best addressed by using a noble gas (xenon or argon) as a fuel.

### Acknowledgments

The particle data used here are from Dr. C.E. McIlwain of the University of California at San Diego. The ion engine experiment was the project of Dr. Robert Hunter and Mr. Robert Bartlett of GSFC, who also provided a great deal of help in the analysis of the data. Dr. Ray Goldstein of NASA/JPL also played an important role in the analysis of the engine operation. This work was supported by NASA/LeRC under NSG-3150, with data taken under NASA/GSFC Contract NAS5-23481.

### References

- <sup>1</sup> DeForest, S.E., "Spacecraft Charging at Synchronous Orbit," *Journal of Geophysical Research*, Vol. 77, 1972, pp. 651-659.
- <sup>2</sup> DeForest, S.E., "Electrostatic Potentials Developed by ATS-5," *Photon and Particle Interactions with Surfaces in Space*, edited by R.J.L. Grard, D. Reidel, Holland, 1973, pp. 263-276.
- <sup>3</sup> Reasoner, D.L., Lennartsson, W., and Chappell, C.R., "Relationship between ATS-6 Spacecraft-Charging Occurrences and Warm Plasma Encounters," *Spacecraft Charging by Magnetospheric Plasmas*, Progress in Astronautics and Aeronautics, edited by A. Rosen, AIAA, New York, Vol. 47, 1976, pp. 89-102.
- <sup>4</sup> McPherson, D.A. and Schober, W.R., "Spacecraft Charging at High Altitudes," *Spacecraft Charging by Magnetospheric Plasmas*, Progress in Astronautics and Aeronautics, edited by A. Rosen, Vol. 47, 1976, pp. 15-30.
- <sup>5</sup> Whipple, E.C. Jr., "Observation of Photoelectrons and Secondary Electrons Reflected from a Potential Barrier in the Vicinity of ATS-6," *Journal of Geophysical Research*, Vol. 81, 1976, pp. 715-719.
- <sup>6</sup> Olsen, R.C., McIlwain, C.E., and Whipple, E.C., "Observations of Differential Charging Effects on ATS-6," *Journal of Geophysical Research*, Vol. 86, 1981, pp. 6809-6819.
- <sup>7</sup> Mandell, M.J., Katz, I., Schnuell, G.W., Steen, P.G., and Roche, J.C., "The Decrease in Effective Photocurrents due to Saddle Points in Electrostatic Potentials Near Differentially Charged Spacecraft," *IEEE Transactions on Nuclear Science*, Vol. NS-25, 1978, p. 1313.
- <sup>8</sup> Kerslake, W.R., Goldman, R.G., and Neiberding, W.C., "SERT II: Mission Thruster Performance and In-Flight Thrust Measurements," *Journal of Spacecraft and Rockets*, Vol. 8, 1971, pp. 213-224.
- <sup>9</sup> Worlock, R.M., James, E.L., Hunter, R.E., and Bartlett, R.O., "ATS-6 Cesium Bombardment Engine North-South Stationkeeping Experiment," *IEEE Transactions on Aerospace and Electronic Systems*, Vol. AES-11, 1975, pp. 1176-1184.
- <sup>10</sup> Goldstein, R. and DeForest, S.E., "Active Control of Spacecraft Potentials at Geosynchronous Orbit," *Spacecraft Charging by Magnetospheric Plasmas*, Progress in Astronautics and Aeronautics, edited by A. Rosen, AIAA, New York, Vol. 47, 1976, pp. 169-181.
- <sup>11</sup> Mauk, B.H. and McIlwain, C.E., "ATS-6 UCSD Auroral Particles Experiment," *IEEE Transactions on Aerospace and Electronic Systems*, Vol. AES-11, 1975, pp. 1125-1130.
- <sup>12</sup> Grard, R.J.L., "Properties of the Satellite Photoelectron Sheath Derived from Photoemission Laboratory Measurements," *Journal of Geophysical Research*, Vol. 78, 1973, pp. 2885-2906.
- <sup>13</sup> Olsen, R.C., "Warms Ions at Midnight," *Transactions, American Geophysical Union*, Vol. 60, 1979, p. 930.
- <sup>14</sup> Komatsu, G.K. and Sellen, J.M. Jr., "A Plasma Bridge Neutralizer for the Neutralization of Differentially Charged Surfaces," *Effect of the Ionosphere on Space and Terrestrial Systems*, edited by J. Goodman, U.S. GPO, Washington, D.C., 1978, pp. 317-321.
- <sup>15</sup> Olsen, R.C., "Modification of Spacecraft Potentials by Thermal Electron Emission on ATS-5," *Journal of Spacecraft and Rockets*, (Sept./Oct.).
- <sup>16</sup> Rawlin, V.K. and Pawlik, E.V., "A Mercury Plasma-Bridge Neutralizer," *Journal of Spacecraft and Rockets*, Vol. 5, 1968, pp. 814-820.
- <sup>17</sup> Ward, J.W. and King, H.J., "Mercury Hollow Cathode Plasma Bridge Neutralizers," *Journal of Spacecraft and Rockets*, Vol. 5, 1968, pp. 1161-1164.